

SUPPLEMENTARY MATERIAL: PART II

Further Results

1 Cross-modal prior

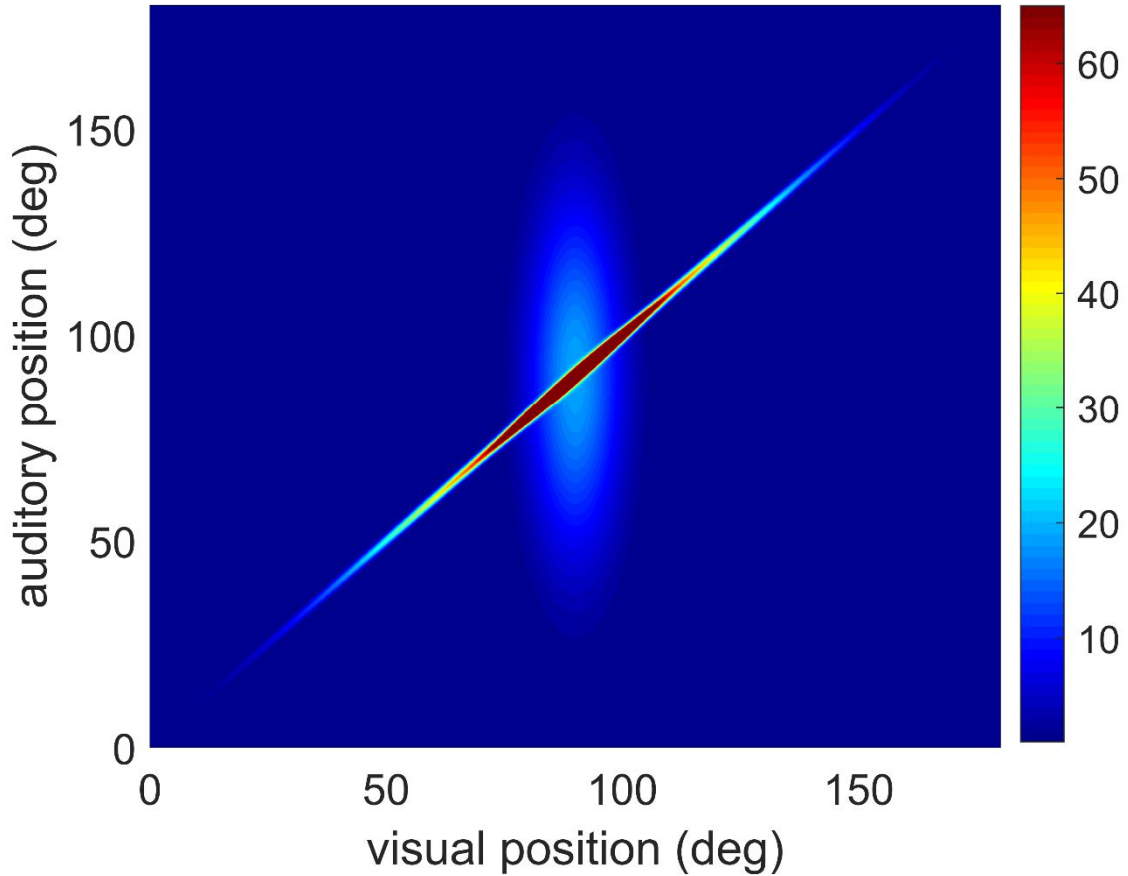


Figure S1 - 2D color map of the joint cross-modal probability (i.e. Eq. (16) in Supplementary Materials part I) obtained using $\beta = 0.5$ (50% probability of independent inputs in cross-modal conditions), $s_V = 7$ deg (standard deviation of the visual unisensory prior), $s_A = 30$ deg ((standard deviation of the visual unisensory prior) and $s_{AV} = 1$ deg (standard deviation of the conditioned probability in case of stimuli originating from the same cause).

2 Correlation among experimental and model data

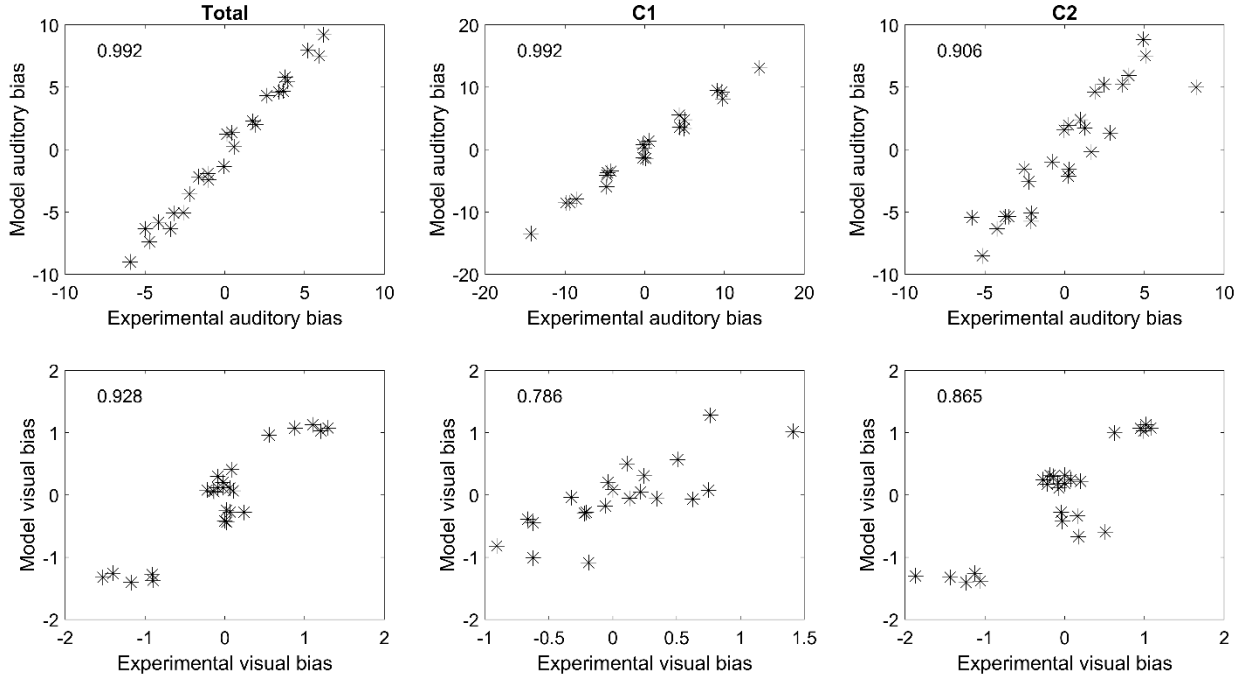


Figure S2 – Correlation among the experimental and model values of the auditory bias (upper line) and the visual bias (bottom line), evaluated in the *high contrast condition* using all data available (first column) and considering just the cases with $C = 1$ (second column) and $C = 2$ (third column). In the figures, only data simultaneously available from both the experimental conditions and model simulations are reported. These data are taken from the six panels in Fig. 5 (for what concerns the auditory bias) and from the six panels in Fig. 6 (for what concerns the visual bias). The value of the correlation coefficient is reported in each panel.

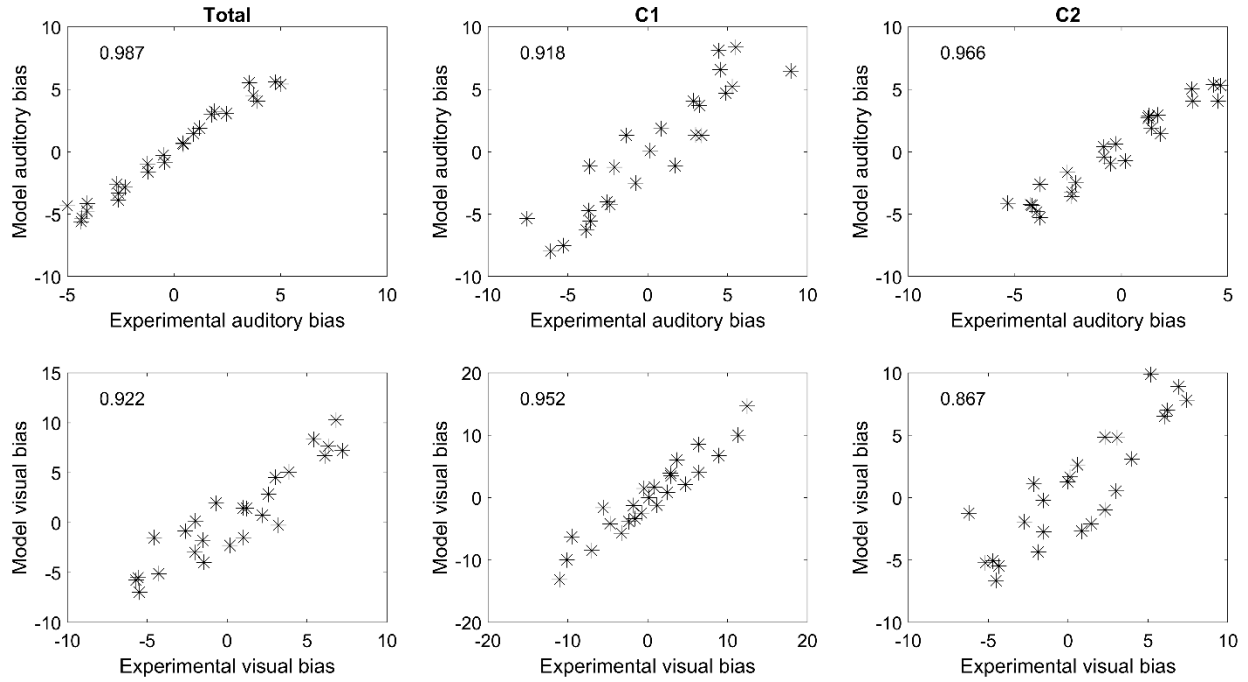


Figure S3 – Correlation among the experimental and model values of the auditory bias (upper line) and the visual bias (bottom line), evaluated in the *low contrast conditions* using all data available (first column) and considering just the cases with $C = 1$ (second column) and $C = 2$ (third column). In the figures, only data simultaneously available from both the experimental conditions and model simulations are reported. These data are taken from the six panels in Fig. 7 (for what concerns the auditory bias) and from the six panels in Fig. 8 (for what concerns the visual bias). The value of the correlation coefficient is reported in each panel.

3 Sensitivity analysis at low-contrast

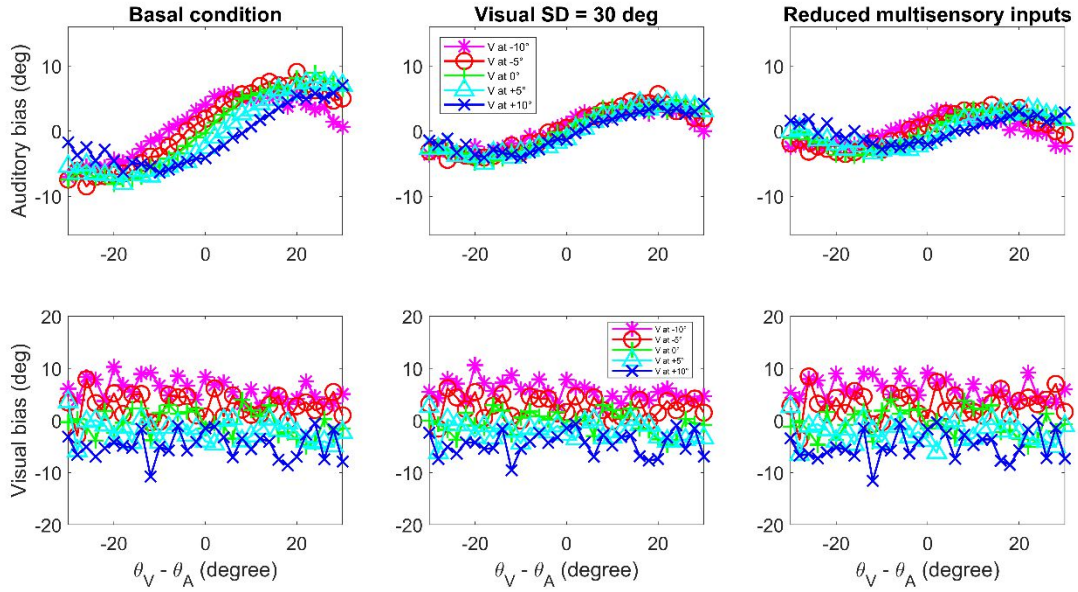


Figure S4 – Dependence of model results on the stimuli experienced during training (i.e., on the *prior probability*) in *low-contrast conditions*. The upper panels show the bias in the perceived position of the auditory stimulus; the bottom panels the bias in the visual perception. The meaning of lines is the same as in Fig. 9. The first column was obtained after Training1 (that is the same used in Figures 2-8). The second column was obtained after a different training (Training2) characterized by a larger spatial arrangement of visual stimuli around the fovea. The third column was obtained after Training3, characterized by a smaller percentage of cross-modal inputs.

4 Synapse changes during re-learning

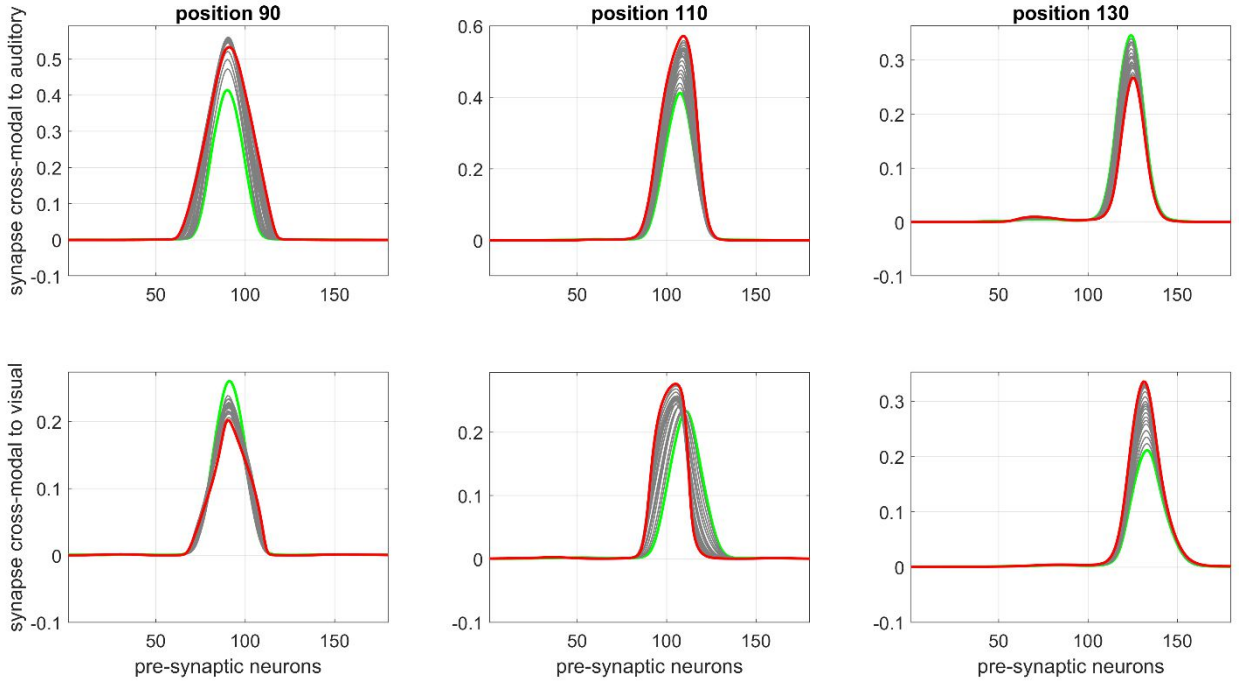


Figure S5 – An example of how cross-modal synapses change during re-learning from a condition with a standard deviation of the visual unisensory prior as large as $s_V = 30$ deg, to a condition with $s_V = 7$ deg (that is the same re-learning illustrated in Fig. 11 of the text). The upper line represents synapses entering into an auditory neuron from all visual neurons in the visual net. The bottom line represents cross modal synapses entering into a visual neuron from all auditory neurons in the auditory net. The green line represents the synapse distribution in the mature configuration before re-learning, whereas the red line is the synapse distribution after re-learning. Gray lines are examples of iterations during the re-learning. As for cross-modal synapses entering auditory neurons, it is evident a reinforcement of the cross-modal input close to the fovea. As for cross-modal synapses entering visual neurons, it is evident a shift of the cross-modal input toward the fovea at intermediate azimuthal positions, and a reinforcement of the visual cross-modal input at more peripheral azimuthal locations.

5 Additional simulations with the lesioned network

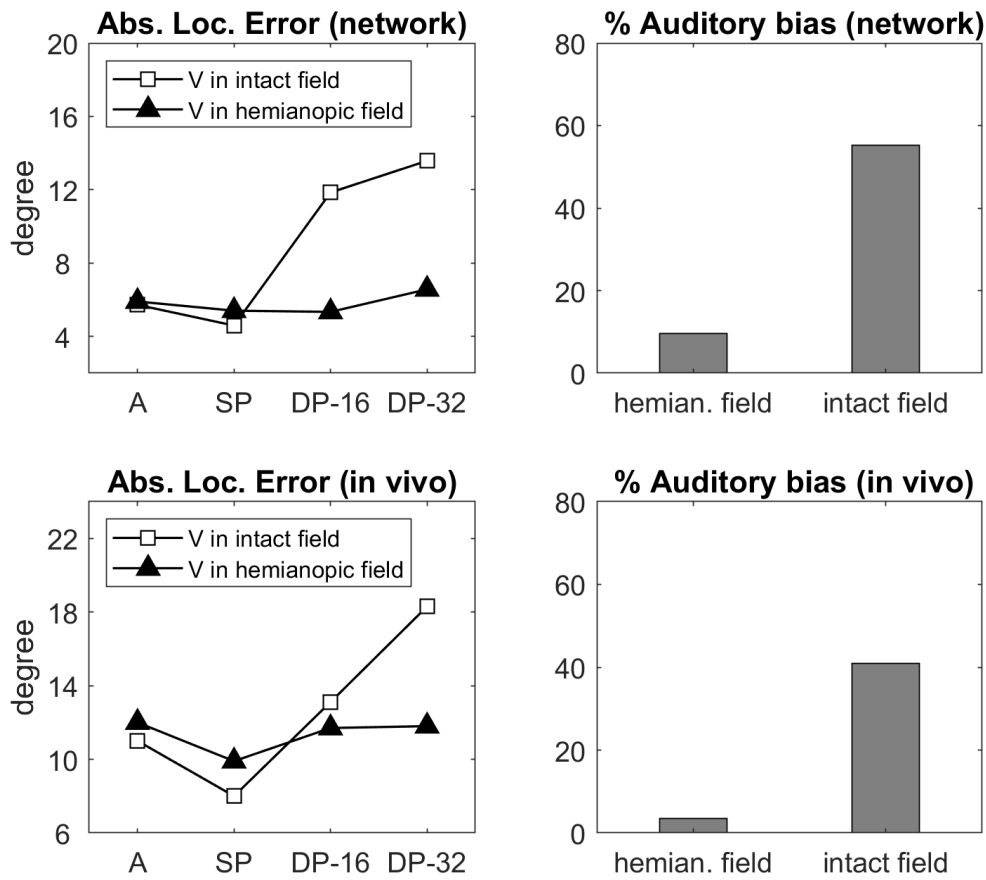


Figure S6 – The lesioned network (90% of damaged neurons in the right visual hemifield) was used to replicate an experiment similar to that performed in hemianopic patients (Leo *et al.*, 2008). Simulated results are shown in the upper plots and in vivo data are redrawn in the lower plots. In the network, a visual stimulus was applied either at -10° (intact hemifield) or at $+10^\circ$ (in the lesioned hemifield) and paired with an auditory stimulus applied at the same spatial position (SP) or at 16° and 32° of spatial disparity (DP16, DP32). The auditory stimuli were presented in unimodal conditions (A), too. The simulations were performed using a visual stimulus with strength 18, an auditory stimulus with strength 36, and in noisy condition (average values are displayed). Plots in the left column show the absolute localization error (absolute difference between the perceived auditory location and the real auditory location) computed in each condition (A, SP, DP16 and DP32) separately for the visual stimulus in the intact and damaged hemifield. Plots in the right column show the percentage of auditory bias $[100 * (\text{perceived auditory location} - \text{real auditory location}) / (\text{actual visual-auditory disparity})]$ in DP16 and DP32 conditions (collapsed together) for the visual stimulus in the intact and damaged hemifield. According to the network (upper plots), a visual stimulus in the intact hemifield slightly reduces the auditory localization error in SP condition and strongly increases auditory mislocalization in DP condition, producing a high ventriloquism effect; conversely, a visual stimulus in the lesioned hemifield has only a weak impact on auditory localization error, and the ventriloquism effect radically declines. These network outcomes display good agreement with the in vivo data (lower plots).